SAN FRANCISCO ESTUARY & WATERSHED SCIENCE
Sponsored by the Delta Science Program and the UC Davis Muir Institute

RESEARCH

Modeling Delta Smelt Distribution for Hypothesized Swimming Behaviors

Edward S. Gross*[1], Josh Korman[2], Lenny F. Grimaldo[3], Michael L. MacWilliams[4], Aaron J. Bever[4], Peter E. Smith[5]

ABSTRACT

Delta Smelt, *Hypomesus transpacificus*, is an endangered pelagic fish native to the San Francisco Estuary. The distribution of Delta Smelt in the estuary shifts landward from low-salinity habitat to freshwater habitat before spawning. This spawning migration often coincides with the first substantial freshwater inflow to the estuary during winter. To accomplish this landward shift in distribution, Delta Smelt are believed to use the tides by swimming to faster-moving currents during flood tides and then repositioning themselves to slower-moving currents to reduce seaward movement on ebb tides. Studies have hypothesized that the swimming behavior of Delta Smelt during this period is influenced by environmental conditions such as salinity and turbidity. The details of these swimming behaviors—including the extent to which flows, salinity, and turbidity affect behaviors and distributions—are uncertain. The spawning migration is of management interest because an increase in observed counts of Delta Smelt at the South Delta water-export facilities has coincided roughly with the spawning migration in many years. In this study, we investigated a range of hypothesized swimming behaviors using a three-dimensional particle-tracking model for water year 2002 during the spawning migration, and compared the predicted distributions of Delta Smelt to distributions inferred from catch data. Our goal was to improve understanding of the influence of Delta Smelt swimming on distribution, and, ultimately, to develop a modeling tool to help management agencies identify conditions associated with entrainment losses. Predictions of Delta Smelt distributions and entrainment varied greatly among behaviors. Without swimming, Delta Smelt would be rapidly transported seaward of Suisun Bay, while continuous tidal migration would move them deep into the interior Delta. These behaviors and a simple turbidity-driven behavior model predicted distributions inconsistent with observations, while more complex behavior rules allowed improved predictions.

SFEWS Volume 19 | Issue 1 | Article 1

https://doi.org/10.15447/sfews.2021v19iss1art3

* Corresponding author: *ed@rmanet.com*

1 Resource Management Associates, Inc.
Walnut Creek, CA 94596 USA

2 Ecometric Research
Vancouver, BC, V6S 1J3 Canada

3 California Department of Water Resources
Sacramento, CA 95814 USA

4 Anchor QEA, LLC
San Francisco, CA 94111 USA

5 California Water Science Center,
US Geological Survey (retired)
Sacramento, CA 94107 USA

KEY WORDS

Delta Smelt, fish movement, entrainment, hydrodynamics, particle-tracking, maximum likelihood

INTRODUCTION

Many fish species undergo synchronous and directed migration movements from one habitat to another during spawning to improve survival of their eggs and/or progeny after hatching (Leggett 1977; Tsukamoto et al. 2009; Binder et al. 2011). Although the timing and direction of spawning movements can vary among individuals within populations (Tsukamoto et al. 2009), behaviors that underlie spawning movements often involve a continuous optimization of physiological and neurological states in response to environmental stimuli (Leggett 1977). For example, ayu (*Plecoglossus altivelis*) spawning migration (upstream movements) responds to changes in water temperature and fish density, resulting in upstream swimming to new habitats, presumably to improve reproductive fitness (Tsukamoto et al. 2009). In contrast, salmon spawning migration behavior is strongly influenced by visual and olfactory cues (Leggett 1997).

Understanding spawning migrations in estuarine ecosystems is challenging because of variable water-quality gradients (Secor and Rooker 2000; Walsh et al. 2013), and fish may only move short distances to spawning habitats (Walsh et al. 2013). In the San Francisco Estuary, the native and endangered Delta Smelt (*Hypomesus transpacificus*) is a small osmerid that exhibits variable life histories. Some individuals are tidal freshwater residents (Hobbs et al. 2019), some move only a few kilometers from low-salinity habitat (1 to 6 psu) to freshwater for spawning (Murphy and Hamilton 2013; Polansky et al. 2017), while others migrate from low-salinity habitat to freshwater habitats many kilometers upstream (Grimaldo et al. 2009; Sommer et al. 2011) or downstream during periods of high freshwater flow (Grimaldo et al. 2009). Of these different life histories, the behavior that puts Delta Smelt at most risk is landward movement to the interior Delta, because of entrainment losses at the water-export facilities for California's two largest water projects: the State Water Project (SWP) and the federal Central Valley Project (CVP) (Figure 1; Kimmerer 2008; Grimaldo et al. 2009).

Entrainment of adult Delta Smelt that enter the interior Delta generally increases with greater water exports, which is indexed by reverse (landward) flow in the two main channels: Old and Middle rivers (OMR; Figure 1), leading to the export facilities (Grimaldo et al. 2009). The CVP and SWP have fish-screening facilities upstream of the major diversions which "salvage" a portion of the fish that reach the facilities. Salvage data can be used to estimate total entrainment losses (mortality) after applying assumptions regarding the efficiency of fish collection and other factors (Kimmerer 2008; Korman et al., this volume). Observed salvage is typically higher under turbid conditions which are often associated with the first large flow event of the season, known as the "first flush" (Grimaldo et al. 2009).

When fish migrate from one habitat to another, three conditions are needed: (1) locomotory ability, (2) orientation ability, and (3) motivation to behave a certain way (Tsukamoto et al. 2009). Each of these has been studied to some extent for Delta Smelt, but understanding of the orientation (direction) of Delta Smelt swimming, and the environmental stimuli that motivate the swimming, remain uncertain. Adult Delta Smelt can swim at 1 to 2 body lengths per second for a prolonged period, and higher speeds for more limited periods (Swanson et al. 1998), which could result in migration speeds as high as $10\,km\,d^{-1}$ in the absence of seaward advection by net flow. However, because seaward advection is substantial over a day, Delta Smelt are believed to use tidal migration ("tidal surfing") to accomplish an inland-directed spawning migration (Sommer et al. 2011). Tidal migration involves fish positioning themselves in faster-moving currents during flood tides, and then repositioning themselves in slower-moving currents to reduce seaward movement on ebb tides. A series of field observations of Delta Smelt during late November of 2012 in the lower Sacramento River indicated Delta Smelt occupied

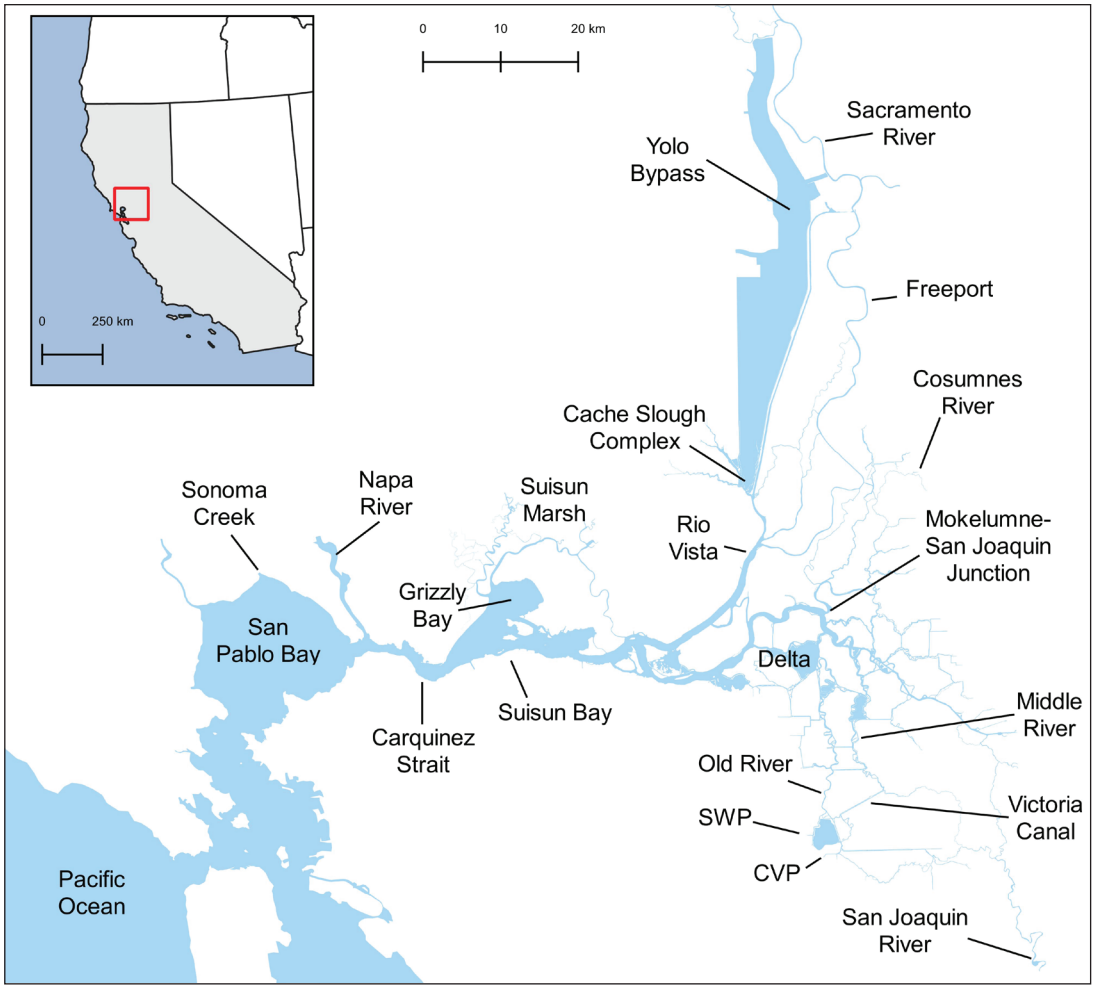

Figure 1 Study area. "SWP" indicates the location of the Harvey O. Banks Pumping Plant of the State Water Project and "CVP" indicates the location of the C.W. Bill Jones Pumping Plant of the Central Valley Project.

the entire water column during flood tides, and were typically observed deeper in the water column and near channel margins on ebb tides (Feyrer et al. 2013). These observations preceded the expected spawning migration of Delta Smelt, so the behavior is associated with pre-migration retention, as opposed to landward migration. Feyrer et al. (2013) conclude that Delta Smelt remaining within preferred turbidity and salinity conditions could explain much of the observed distribution. Bennett and Burau (2015) reported on two other field sampling studies from January 2010 and December 2011 where Delta Smelt were sampled in the lower Sacramento and San Joaquin rivers during first-flush events. In these studies, water current velocities and turbidity levels were measured concurrently with the Delta Smelt sampling. The authors observed strong tidal variability in the lateral distribution of Delta Smelt, which were caught consistently at the shoal-channel interface during flood tides, and near the shoreline using beach seines during ebb tides in the turbid Sacramento River. Delta Smelt catches were rare in the clearer San Joaquin River. Bennett and Burau (2015) hypothesized that the observed tidal variability in distribution was related to the tidal variability in turbidity gradients during and after a large flow event.

Delta Smelt distribution has been modeled using several approaches, including statistical approaches (e.g., Polansky et al. 2017), particle-

https://doi.org/10.15447/sfews.2021v19iss1art3

tracking models (e.g., Sommer et al. 2011) and individual-based models (e.g., Rose et al. 2013). The work documented here is the first published three-dimensional (3-D) simulation of Delta Smelt movement using a particle-tracking model with behavior rules. As in the work of Goodwin et al. (2014) for salmon, the Delta Smelt swimming behavior of the modeled individuals (particles) is updated at short time intervals (time-steps) in response to environmental stimuli, including hydrodynamic properties, salinity, and turbidity. The only difference among the scenarios evaluated in this work is the behavior rules that are applied. We refer to the combination of the particle-tracking model and a set of behavior rules as a "behavior-driven movement model" (BMM). The BMMs explored here were informed by concepts of swimming behavior in the literature (reviewed above), guidance from the Collaborative Adaptive Management Team (CAMT) Delta Smelt Scoping Team (DSST), and exploratory simulations conducted during this study. A much larger set of BMMs were explored than the six documented here, with a subset documented in Gross et al. (2018). We chose the BMMs discussed here because they range from simple to moderately complex, and include some of the best performing BMMs discussed in Gross et al. (2018), based on comparisons to SKT catch and Delta Smelt salvage.

All predictions of spatial distributions use the same initial spatial distribution and survival to isolate the effect of the behavior rules on predicted distribution. These simulations of movement from release locations provide a foundation for the companion paper (Korman et al., this volume), which includes fitting parameters and explores multiple assumptions regarding survival and salvage efficiency that determine the fit of model predictions to the data.

Representation of Delta Smelt swimming behavior may allow improved prediction of entrainment risk and improved understanding of the contribution of entrainment to the observed decline in indices of abundance. A predictive capability is particularly important in the current environment of very low abundance and catch, because survey and salvage data may no longer be sufficient to identify periods of high entrainment. The evaluation of BMMs documented here along with the larger set of results in Gross et al. (2018) is a step toward a predictive model which, if substantially improved and validated, could provide real-time predictions of entrainment and be used to adjust water-export regimes.

We selected water year of 2002 as the study year because of the availability of fish survey data to support the analysis and relatively higher observed catch compared with other survey years. As a result of the combination of low inflow to the Delta and substantial flow toward the export facilities, we expect the study year of 2002 to have substantial entrainment risk. Kimmerer (2008) estimated proportional entrainment losses (PEL) of 15% of the Delta Smelt population in 2002 with a 95% confidence interval of 5% to 24%. Uncertainties to this estimate were discussed in Miller (2011) and Kimmerer (2008), and Kimmerer (2011) revised the PEL estimate to 13% for 2002.

METHODS

Study Area

The study area is the upper San Francisco Estuary (the estuary) including Carquinez Strait, Suisun Bay, Suisun Marsh, and the Sacramento-San Joaquin Delta (Figure 1). The climate is Mediterranean, with highly variable precipitation in winter and spring, and consistently dry summer and fall. The majority of inflow to the estuary is from the Sacramento River in the North Delta, and the largest exports for California's SWP and the federal CVP are located in the South Delta (Figure 1), on the opposite side of the Delta. These exports can create a southward net flow across the Delta toward the pumps, most notably in Old River and Middle River (Grimaldo et al. 2009). The difference between freshwater inflows to and diversions from the Delta dictate the net flow of water from the Delta, termed "Delta Outflow."

The estuary has mixed diurnal and semidiurnal tides, with pronounced spring-neap variability

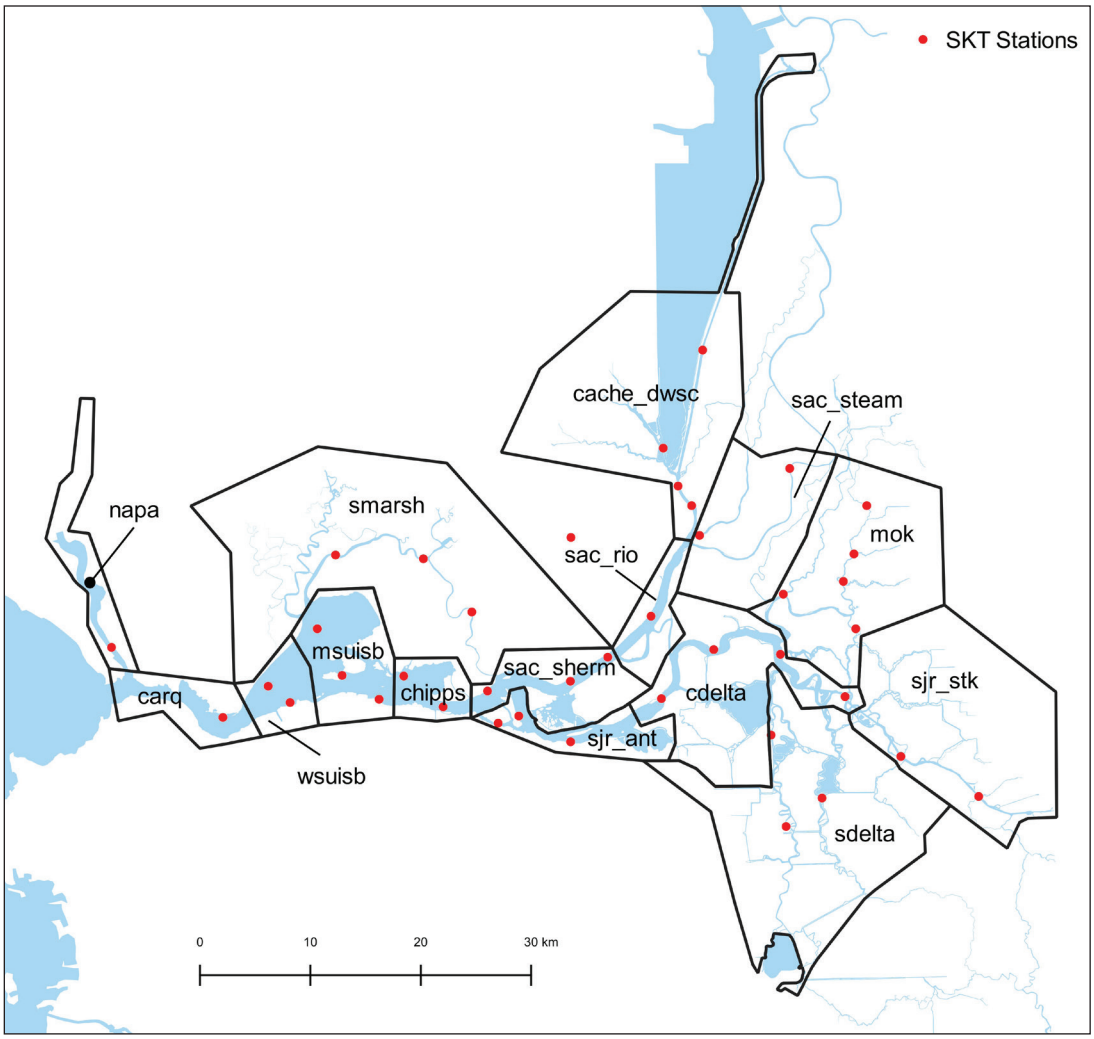

Figure 2 Spring Kodiak Trawl (SKT) station locations (*red points*) and regions (*black outlines*) defined for adult Delta Smelt analysis. See Table 1 for definition of region names.

(Cheng et al. 1993). The Delta is typically fresh, though brackish water may intrude in summer and fall as a result of low Delta outflow, and Carquinez Strait and Suisun Bay are typically partially mixed with tidally-variable stratification through most of the year.

The study year (2002) was the first year of the Spring Kodiak Trawl (SKT) survey (Figure 2) and was a year before a sharp decline that occurred in the Delta Smelt population indexes (Sommer et al. 2007; Baxter et al. 2010). The substantial catches of Delta Smelt collected in the SKT surveys in 2002 are useful for defining the monthly distributions of Delta Smelt. Significant numbers of Delta Smelt were collected in the salvage sampling (a proxy for numbers of entrained fish) at the two water project fish facilities in water year 2002. Salvage was first recorded on December 11, 2001 at the CVP (Tracy) fish facility and continued at both facilities through the end of January 2002; relatively few additional adult Delta Smelt were salvaged later (in February and March) (Figure 3). During the 3-day period from January 2 through 4, 2002, the total combined salvage from both the CVP and SWP fish facilities spiked considerably, exceeding daily combined totals of 800 Delta Smelt each day (Figure 3).

https://doi.org/10.15447/sfews.2021v19iss1art3

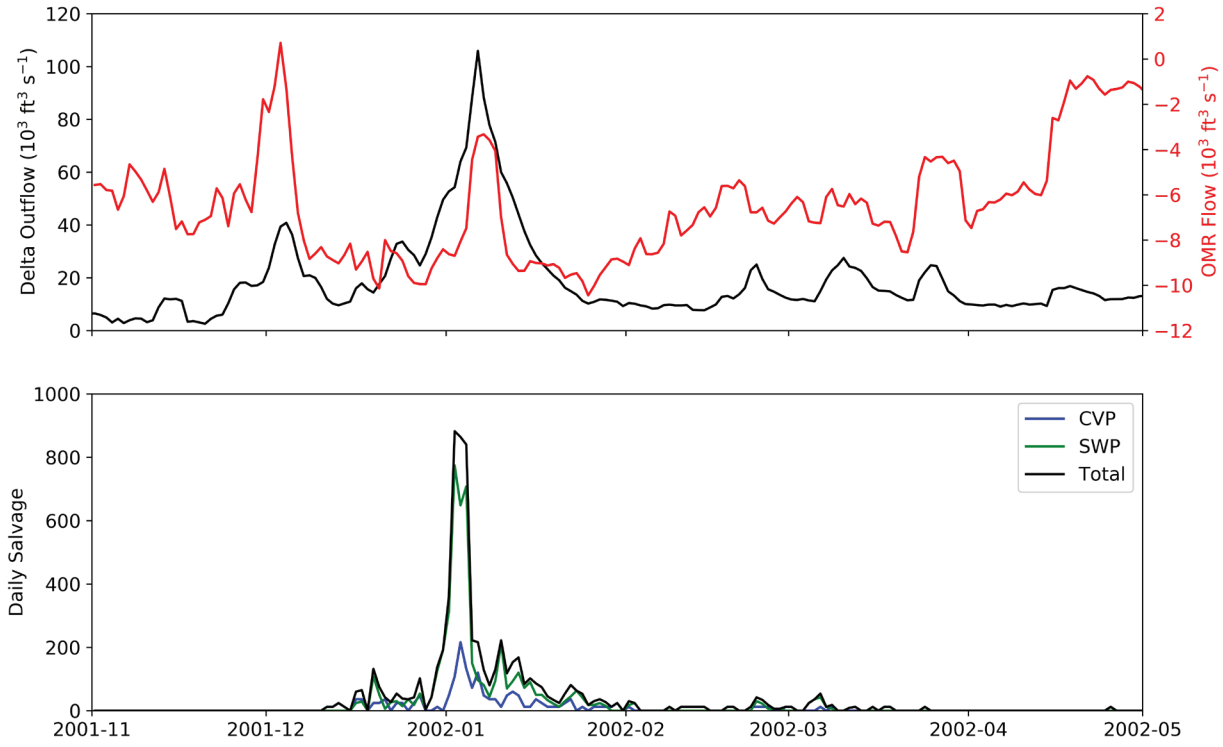

Figure 3 (**A**) Net Delta Outflow and combined Old and Middle River (OMR) flow with negative values indicating southward flow toward export facilities; and (**B**) daily salvage data in numbers of adult Delta Smelt from the Skinner Fish Facility at the SWP and the Tracy Fish Collection Facility at the CVP.

Water year 2002 (October 1, 2001 through September 30, 2002) was classified as a dry year in both the Sacramento and San Joaquin River valleys (CDWR 2016), although significant wintertime pulses of inflow occurred on both rivers. Net Delta Outflow first increased to about 40,000 cfs on December 4, 2001, and then peaked at just over 100,000 cfs about 1 month later on January 6, 2002; three small (< 30,000 cfs) inflow pulses occurred subsequently, one in late February and two in March (Figure 3). 2002 was before the implementation of management actions to limit the southward net flows through the Old and Middle River (OMR) corridor. During most of the winter of 2002, the daily combined reverse flow in Old River and Middle River significantly exceeded the maximum flow of 5,000 cfs allowed under "Reasonable and Prudent Alternative" (RPA) Action 2 of the US Fish and Wildlife Service Biological Opinion (USFWS 2008), first instituted in 2009. Daily-averaged OMR reverse flows equaled or exceeded 10,000 cfs during 13 days within the months of December and January of water year 2002 (Figure 3).

Delta Smelt Trawl Data

Our study uses Delta Smelt catch data from two California Department of Fish and Wildlife surveys: the Spring Kodiak Trawl (SKT) and the Fall Midwater Trawl (FMWT). The SKT survey began in 2002 and samples adult Delta Smelt once per month between January and May at 40 stations (Figure 2). Only 3 months of survey data (January through March) are available for water year 2002. The FMWT survey samples sub-adult Delta Smelt once monthly at 122 station locations from September through December dating back to 1967. For more information on both surveys see Honey et al. (2004).

We used the catch data summed across all FMWT surveys from September to December of 2001 to define the initial distribution of Delta Smelt. We use the SKT data to estimate monthly regional

Table 1 List of regions with abbreviated names, associated water volume within 4 m from the surface, and fraction of initial abundance of the total population by region estimated from the FMWT survey data from 2001

Region name	Abbreviation	Habitat volume (m^3)	FMWT fraction
Napa River	napa	3.05E+07	0.000
Carquinez Strait	carq	7.58E+07	0.000
West Suisun Bay	wsuisb	8.08E+07	0.004
Mid Suisun Bay	msuisb	1.54E+08	0.035
Suisun Marsh	smarsh	3.39E+07	0.027
Chipps Island	chipps	6.12E+07	0.026
Sacramento River near Sherman Lake	sac_sherm	7.76E+07	0.415
Sacramento River near Rio Vista	sac_rio	4.71E+07	0.268
Cache Slough and SDWSC	cache_dwsc	7.78E+07	0.189
Sacramento River and Steamboat Slough	sac_steam	1.86E+07	0.000
San Joaquin River near Antioch	sjr_ant	7.22E+07	0.023
Central Delta and Franks Tract	cdelta	1.43E+08	0.012
North and South Forks Mokelumne River	mok	3.80E+07	0.000
San Joaquin near Stockton	sjr_stk	4.00E+07	0.000
South Delta	sdelta	9.74E+07	0.000

abundances that we then compare with predicted abundances from the behavior models.

We defined 15 contiguous regions (Figure 2) so that each one included at least one SKT survey sampling station. In some cases, we located boundaries to distinguish regions that are geometrically or hydrodynamically distinct. For example, we define a Suisun Marsh region instead of including Suisun Marsh in the Suisun Bay region. Some portions of the Delta which are not considered habitat typically occupied by adult Delta Smelt (Sommer and Mejia 2013) were not included in any region. Excluded areas include the portion of the Delta north of the Delta Cross Channel Gates, and the portion of the South Delta south of Victoria Canal. We estimated Delta Smelt habitat volume as the water volume within 4 meters of the water surface in each region (Table 1), as has been assumed in previous work (Kimmerer 2008). We used a water surface elevation of 1.25 m NAVD88, corresponding to mean sea level (MSL) at Antioch, in the calculation.

Hydrodynamic Model

The UnTRIM San Francisco Bay-Delta model (UnTRIM Bay-Delta model) is a 3-D hydrodynamic model of San Francisco Bay and the Sacramento-San Joaquin Delta (MacWilliams et al. 2015) that we used to predict water velocity, depth, and salinity over space and time. The UnTRIM Bay-Delta model extends from the Pacific Ocean through the entire Sacramento-San Joaquin Delta (Figure 4), using an unstructured computational mesh that gradually varies the grid-cell sizing, beginning with large grid cells in the Pacific Ocean and transitioning to much smaller grid-cell sizes in the narrow channels of the Sacramento-San Joaquin Delta. In the South Delta, most channels are resolved using 4 to 10 cells across the width of the channel, with edge lengths on the order of 15 to 20 meters in many channels in the South Delta (See Figure 4 in MacWilliams et al. 2015). The UnTRIM Bay-Delta model was applied together with the Simulating WAves Nearshore (SWAN; SWAN Team 2009) wave model and the SediMorph sediment-transport and seabed-morphology model (Malcherek 2001; BAW 2005; Malcherek and Knock 2006), as a fully coupled hydrodynamic-wave-sediment-transport

https://doi.org/10.15447/sfews.2021v19iss1art3

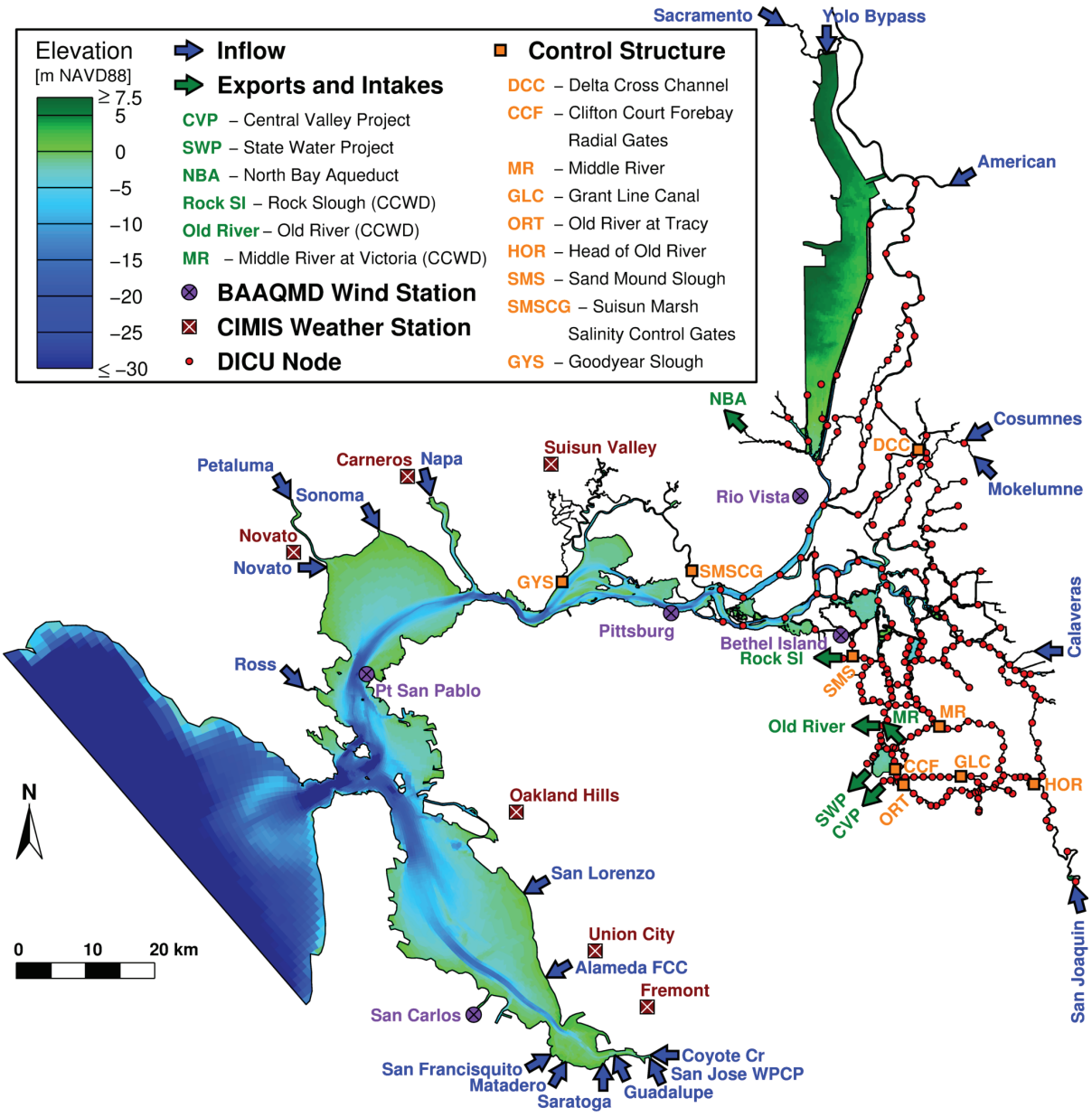

Figure 4 UnTRIM San Francisco Bay-Delta model domain, bathymetry, and locations of model boundary conditions, which include inflows, export facilities, intakes for the Contra Costa Water District (CCWD), wind stations from the Bay Area Air Quality Management District (BAAQMD), evaporation and precipitation from California Irrigation Management Information System (CIMIS) weather stations, Delta Island Consumptive Use (DICU), and flow control structures

model (Bever and MacWilliams 2013; Bever et al. 2018). More specifics on the hydrodynamic-wave-sediment-transport model are provided in Bever and MacWilliams (2013).

Sediment-Transport and Turbidity Model

A mechanistic sediment-transport model was applied to estimate 3-D distribution of suspended-sediment concentration (SSC) and turbidity over time. We simplified the continuously varying grain size distribution to represent the most dominant constituents, as has previously been

done in 3-D sediment-transport modeling of San Francisco Bay (Ganju and Schoellhamer 2009; van der Wegen et al. 2011; Bever and MacWilliams 2013; Bever at al. 2018). Sediment-transport calculations included four sediment classes, representative of silt, flocculated silts and clays (flocs), sand, and gravel. Additional details of the sediment classes are provided in Bever et al. (2018). We used more than 1,000 observed surface grain size distributions to generate a realistic initial grain size distribution on the bed of the entire San Francisco Bay-Delta system, as described in Bever and MacWilliams (2013). Suspended sediment was supplied through river input to the Sacramento-San Joaquin Delta, the North Bay, and the South Bay. Sediment was supplied to the Delta by the Sacramento, San Joaquin, Cosumnes, and Mokelumne rivers and the Yolo Bypass, as described in Bever and MacWilliams (2013), representing nearly 100% of the sediment inflow to the Delta (Wright and Schoellhamer 2005).

Because the model predicts SSC and not turbidity (nephelometric turbidity units [NTU]) directly, we converted predicted total SSC (the sum of all four sediment classes) to turbidity using a conversion curve developed by comparing SSC data to turbidity data (USGS 2015), similar to the conversions described in Bever et al (2018). In this study, we used a single SSC-to-turbidity conversion curve based on data from the Sacramento River at Freeport from October 2010 to February 2015 to convert SSC to turbidity using Equation 1:

$$T_p = C_1 S^3 + C_2 S^2 + C_3 S + C_4 \quad (1)$$

where T_p is the predicted turbidity (NTU), C are conversion coefficients, and S is the predicted SSC (mg L^{-1}).

The conversion coefficients were –0.000001582, 0.001635570, 0.466618932, and –1.551583359, respectively. Although there is variability in SSC to turbidity curves throughout the system (Bever et al. 2018), we used a single SSC-to-turbidity conversion in this study to ensure artificial spatial gradients in the turbidity field were not introduced by spatial heterogeneity in the SSC-to-turbidity conversion curves. We chose this approach because turbidity gradients were one of the triggers used in some BMMs. In general, the use of the single conversion curve based on data from the Sacramento River at Freeport results in lower predicted turbidity in the South Delta than when spatially varying conversion curves are applied.

Very little observed data exist to validate the spatial patterns in modeled turbidity during the 2002 study period, so turbidity validation was conducted for a similar period during 2010 when more extensive turbidity observations were available for model validation. Bever and MacWilliams (2013) and Bever et al. (2018) provide validations of the overall sediment-transport and turbidity model, and here we present a model-data comparison map of turbidity during 2010 and compare it to a similar period during 2002.

Particle-Tracking Model

Particle movement is driven by hydrodynamic predictions of 3-D velocity and vertical eddy diffusivity from UnTRIM (MacWilliams et al. 2015) on a 15-minute interval. The 3-D FISH particle-tracking model (FISH–PTM; Ketefian et al. 2016) represents advective and diffusive transport processes at the scale of hydrodynamic grid resolution. Particle advection is computed by an analytical integration of a linear velocity field within each cell (Ketefian et al. 2016). The advection approach avoids a common particle-tracking artifact that causes artificial aggregation of particles (Ketefian et al. 2016). Diffusion is represented by the Milstein scheme (Milstein 1974) as recommended in Gräwe et al. (2012), and the time-step for diffusion is specified following Shah et al. (2013).

Approximately 12,000 uniformly distributed particles were released in each region (Figure 2) on December 5, 2001 from 6:00 am to 6:00 pm for each BMM. The uniform distribution of particles within a region does not imply a uniform distribution of Delta Smelt across regions because

https://doi.org/10.15447/sfews.2021v19iss1art3

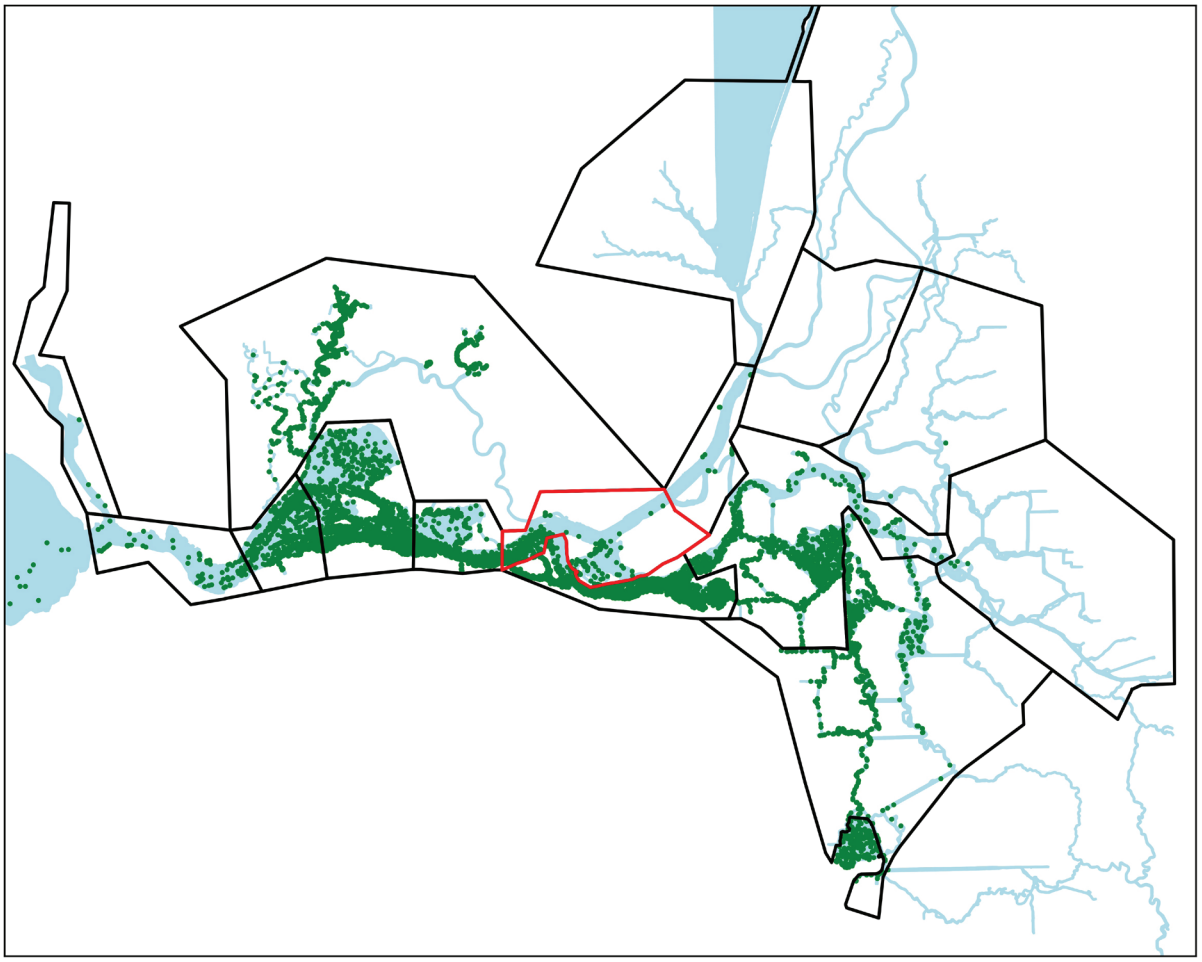

Figure 5 Predicted distribution of particles on January 8, 2002 (during the first SKT survey in 2002) based on releases in the Sacramento River near Sherman Lake region (*red outline*) on December 5, 2001 for behavior-driven movement model (BMM) TpsHt

of the region-specific scaling of the number of fish represented by each particle (super-individual), as will be described subsequently. We chose this date to correspond to the first substantial inflow of the water year. Each particle was tracked at a 5-minute interval until April 17, 2002. When the particle-tracking time is in-between hydrodynamic output intervals saved from UnTRIM, the 3-D hydrodynamic velocity is linearly interpolated in time. We analyzed the regional distribution of particles released from each region for each day during the simulation period, and summarized the distribution as a set of "connectivity matrices" (Paris et al. 2007). We refer to the entire set of these matrices for all release regions and days as the movement array. We include entrainment losses and domain losses that result from transport outside the defined regions in the movement array. For example, to estimate one row of a movement array, corresponding to the Sacramento River near Sherman Lake source region's particle distribution on Jan 8, 2002, we count the particles present in each region (Figure 5), the particles located outside of defined regions, and the particles entrained, and then normalize each count by dividing by the total number of particles released. Entrained particles were tracked by the model to the point when they passed through the louvers at either of the two fish facilities. Movement of particles in Clifton Court Forebay (CCF) of the SWP was simulated by the model. Particles are considered entrained when they reach the location of the Skinner Fish Facility at the exit from CCF.

Representation of Delta Smelt Swimming Behaviors

The velocity of each particle, representative of individual fish, in the particle-tracking model is the summation of the hydrodynamic velocity vector and a swimming vector:

$$\vec{u} = \vec{u}_h + \vec{u}_b \quad (2)$$

where $\vec{u}$ is the 3-D vector of fish velocity over ground, $\vec{u}_h$ is the hydrodynamic velocity, and $\vec{u}_b$ is the swimming (behavior) velocity. The hydrodynamic velocity associated with a particle is linearly interpolated inside the cell to the particle position by the method of Ketefian et al. (2016). The swimming velocity and other properties associated with each particle are updated at a 5-minute interval.

We consider multiple types of environmental stimulus. The simplest is the instantaneous and local value of an environmental property, such as velocity, turbidity or salinity. Another possible stimulus is a local spatial gradient of an environmental property, for example a velocity shear (Goodwin et al. 2014). A third type of stimulus is the acclimatized value of a variable (Goodwin et al. 2014), which can be modeled as a weighted average of conditions over time using:

$$I_a(t) = (1 - m_a) I(t) + m_a I_a(t-1) \quad (3)$$

where $I(t)$ is the instantaneous intensity of the stimulus, $I_a(t)$ is the acclimatized intensity of an environmental stimulus at time t (seconds), and m_a is a dimensionless parameter that determines the time-scale of acclimatization (Goodwin et al. 2014). Larger values of m_a result in slower acclimatization and therefore stronger effects of past conditions. In general, the perceived intensity $I(t)$ relates to the sensory capabilities of a species, and can have a nonlinear relationship to environmental properties (Goodwin et al. 2014). For simplicity, we use the environmental properties (e.g., salinity) interchangeably with the perceived intensity $I(t)$. More general relationships between environmental properties and sensory perception of Delta Smelt could be explored in the future. A fourth type of stimulus is the perceived change from the acclimatized intensity of the stimulus:

$$E(t) = \frac{I(t) - I_a(t)}{I_a(t)} \quad (4)$$

Using these types of stimuli, we developed "behavior rules" for the BMMs that can incorporate multiple criteria to result in a swimming response. Swimming responses to stimuli can also have specified persistence. For example, once triggered, a behavioral response could be assumed to persist for 24 hours.

All BMMs involve some simplifying assumptions. Responses are driven by properties estimated from the hydrodynamic model at the location of each particle, including hydrodynamic velocity, water depth, salinity, turbidity, and distance to shore. Responses are deterministic, and thresholds for responses do not vary among individuals. The behavior rules are static during the simulation period, so the rules do not represent transition from a spawning migration behavior to a staging behavior before spawning. While this framework necessarily simplifies actual behaviors, it allows great flexibility and a large parameter space of behaviors to explore. More complex behavior rules, including those applied by Goodwin et al. (2014) to salmon, allow stochastic responses, which introduce additional parameters. Though more complex behaviors are more consistent with understanding of fish cognition, we believe that increased confidence in the environmental stimuli and swimming responses of Delta Smelt should be achieved before more complexity is added.

https://doi.org/10.15447/sfews.2021v19iss1art3

Specific Delta Smelt Swimming Behavior Rules

We simulated six different behavioral rules (Table 2).

1. **Passive (P):** Individuals have no swimming velocity and move based only on the hydrodynamic velocities. This passive BMM acts as a control, to allow examination of how specific active swimming behaviors influence distribution and salvage relative to fish simply drifting as passive particles.

2. **Turbidity seeking (St):** Individuals swim at 8 cm s^{-1} in the direction of increasing turbidity. The justification for this behavior is that Delta Smelt distributions are known to be associated with turbid water (Feyrer et al. 2007; Nobriga et al. 2008). Bennett and Burau (2015) discuss a concept whereby turbidity gradients guide the direction of Delta Smelt swimming.

3. **Tidal migration (T):** Individuals migrate laterally with the tides following a strategy discussed in Feyrer et al. (2013), Bennett and Burau (2015) and Sommer et al. (2011). It is a strategy by which Delta Smelt may facilitate their landward spawning migration during first flush. In this BMM, individuals swim toward shallower water during ebb tide and deeper water during the flood tide. Individuals swim toward deeper water at 8 cm s^{-1} during flood and toward shallower water at 8 cm s^{-1} during ebb. Eight cm s^{-1} is less than two body lengths per second for adult Delta Smelt, which is a realistic sustained swimming speed (Swanson et al. 1998). When individuals are within 10 m of the shoreline on ebb, they behave as passive particles until the tide changes.

4. **Tidal migration when salinity greater than 1 psu (Ts):** Individuals perform the "tidal migration" behavior described, but only in salinity greater than 1 psu. Once initiated, the tidal migration behavior persists for 24 hours even if salinity drops below 1 psu. This persistence ensures that the tidal migration continues through all phases of the tidal cycle, not only on flood or ebb.

5. **Tidal migration when perceived salinity is increasing (Tps):** Individuals perform the "tidal migration" behavior when the perceived change in salinity according to Equation 4 exceeds a threshold value of 0.5 psu. Equation 3 is used to estimate the perceived salinity using an m_a of 0.995. Once initiated, the tidal migration behavior persists for 24 hours even if the perceived increase in salinity drops below the threshold value.

6. **Tidal migration when perceived salinity is increasing, holding in turbid water (TpsHt):** Individuals follow the same tidal migration rules as Tps and additionally, while tidal migration is not active, swim toward shallow water during ebb tide when turbidity > 12 NTU and local depth is greater than 4 m. Since the turbidity-triggered behavior shifts distribution toward shallower and often relatively quiescent locations, we refer to it as a "holding" behavior.

Table 2 Abbreviationa and brief description of behaviors evaluated

Behavior number	Description	Abbreviation
1	Passive	P
2	Turbidity seeking	St
3	Tidal migration	T
4	Tidal migration when salinity > 1 psu	Ts
5	Tidal migration when perceived salinity is increasing	Tps
6	As above, plus holding when turbidity > 12 NTU	TpsHt

The BMMs included here do not comprehensively span Delta Smelt swimming behavior concepts. For example, a notable concept is that high turbidity may be the cue for Delta Smelt tidal migration, and an associated concept is that Delta Smelt utilize a behavior such as a reverse tidal migration to exit regions of low turbidity. St is

the simplest model we explored using turbidity cues. More complex turbidity-guided behaviors could use acclimatized turbidity, perceived change in turbidity, or only influence behavior in a limited range of turbidity or turbidity gradients. While we have chosen this simple turbidity-seeking behavior rule here, we also explored additional variants of turbidity-driven behaviors, some of which are documented in Gross et al. (2018).

Regional Abundance Model

The estimate of observed regional abundance for each monthly survey is simply determined by multiplying the mean catch density for the region and survey by the region volume within 4 meters of the water surface (Table 1). The predicted regional abundance over time is determined by the initial distribution of particles, predicted movement rates among regions, and survival rate as in Korman et al (this volume). The equation for predicted regional abundance ($N_{i,d}$) is

$$N_{i,d} = A \bullet \phi^{d} \sum_{j}^{nsource} N_{j,d=0} \lambda_{j,i,d} \quad (5)$$

Where A is the total initial abundance across regions, ϕ is daily survival rate, d is simulation day, $nsource = 15$ source regions, $N_{j,d=0}$ is the initial regional abundance in source region j, and $\lambda_{j,i,d}$ is the proportion (fraction) of particles from source region j located in region i on day d predicted by the BMM. A is specified as 4.04 million and ϕ is specified as 0.978, which were estimated parameters from Korman et al. (this volume) under the assumptions of constant survival and salvage expansion factors over time. Survival and initial abundance parameters are fixed at constant values so that they are identical for all BMMs, to facilitate the comparison of spatial distribution across BMMs.

RESULTS

Hydrodynamics and Sediment Transport

The depth-averaged predicted salinity was time-averaged over the duration of the first SKT survey in 2002 (January 7 through 10; Figure 6). Three locations were predicted to have time-averaged depth-averaged salinity between 0.5 and 6 psu during this time: Grizzly Bay, Carquinez Strait and lower Napa River, and San Pablo Bay. The 1-psu isohaline was located in eastern Carquinez Strait, inner Grizzly Bay, and close to the Sonoma Creek inflow. Salinity was decreasing from before January 7 to after January 10, 2002. The quickly decreasing salinity resulted in a patch of relatively higher-salinity water in Grizzly Bay (greater than 0.5 psu) that had not freshened as much as the surrounding portions of Suisun Bay (Figure 6). After the January 7 to 10, 2002 time-period, the salinity throughout Grizzly Bay dropped below 0.5 psu.

Turbidity is highly variable throughout the Bay-Delta over both time and space. A turbidity model to data comparison is focused on December 2010 because of greater data availability in 2010 than 2002. Predicted surface turbidity highlights the complex spatial patterns that occur throughout the Delta as a result of Delta-wide gradients in turbidity combining with complex junction and mixing dynamics. Figure 7 shows the predicted and observed surface turbidity during ebb tide on December 21, 2010 at 01:00 hours with high inflows of freshwater and sediment from the Sacramento River, and relatively low sediment loads from the San Joaquin River to the south. Comparing the predicted turbidity (*map colors*) to the observed turbidity (*colored circles*) demonstrates that the predicted turbidity accurately represented the Delta-wide spatial patterns in turbidity at this time. The Delta-wide turbidity gradient of higher turbidity in the Sacramento River and North Delta than in the South Delta is evident. Complex hydrodynamics near junctions where high turbidity and low turbidity water mix result in sharp turbidity gradients. Similar overall patterns in turbidity were also predicted during the study period in 2002, with higher predicted turbidity in the Sacramento and San Joaquin rivers during 2002

https://doi.org/10.15447/sfews.2021v19iss1art3

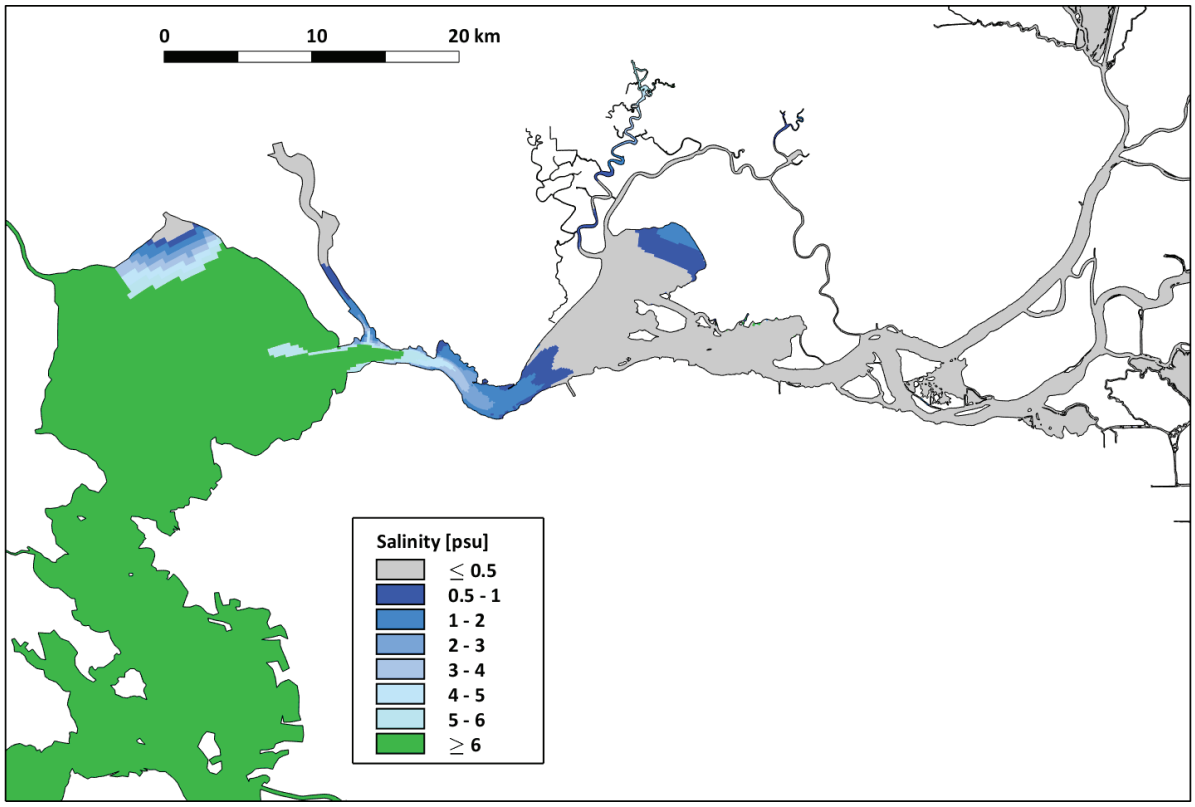

Figure 6 Time- and depth-averaged salinity from January 7 through 10, 2002

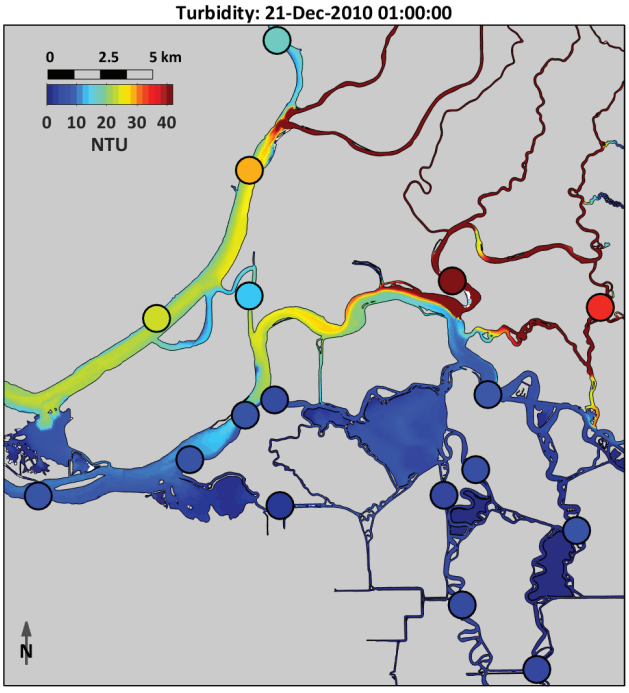

Figure 7 Predicted surface turbidity (*map*) and observed surface turbidity (*filled circles*) on December 21, 2010 at 01:00

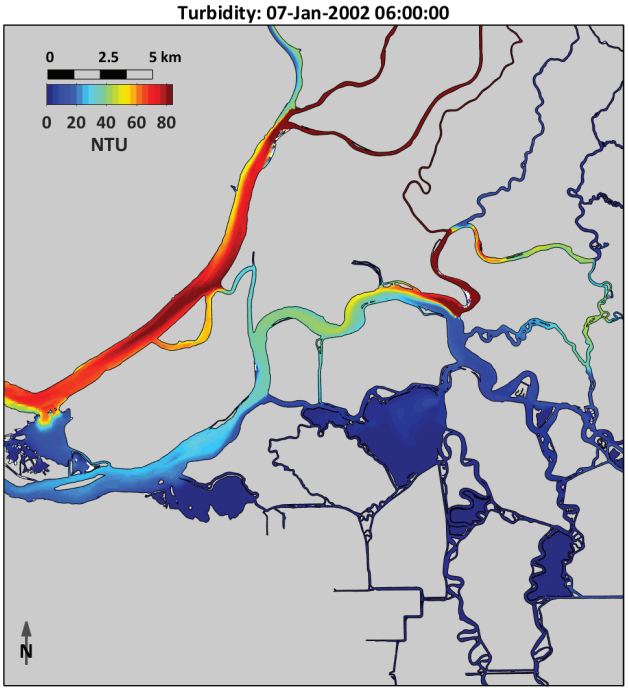

Figure 8 Predicted surface turbidity on January 7, 2002 at 06:00. Note the color scale is twice as high as in Figure 7.

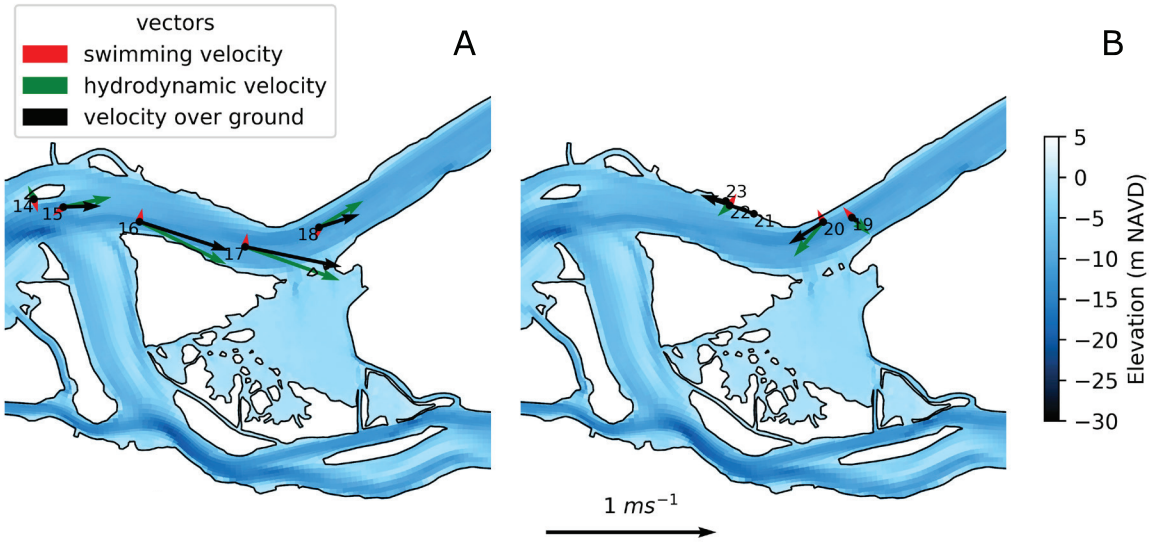

Figure 9 Hourly positions, swimming velocity, hydrodynamic velocity, and velocity over ground for a single particle during (**A**) flood tide and (**B**) ebb tide on December 5, 2001. The hour is labelled next to each set of velocity vectors.

(Figure 8) than 2010 (Figure 7). Although there are not sufficient turbidity measurements from 2002 to directly compare to the model's turbidity predictions as was done for 2010 in Figure 7, this overall gradient is consistent with available measurements of Secchi depth from the FMWT survey during January 2002.

Particle Tracking

Instantaneous movement of individuals is dominated by tidal currents, with typical tidal excursions of 5 to 10 km. The effect of the different behavior rules in BMMs on particle location accumulates over multiple tidal cycles. For example, the tidal migration BMM (T) leads to a net landward displacement over a tidal cycle (Figure 9). During periods of high freshwater inflow, tidal migration may not overcome net seaward flows in some regions, potentially resulting in a seaward shift in distribution.

At the end of the 133-day simulation period, particle locations were broadly classified as lying either within the domain defined by the regions in Figure 2, or seaward or landward of that domain. Particles that were entrained were also counted. Passive (P) and turbidity-seeking (St) BMMs led to seaward domain losses from most regions (Figure 10). The tidal migration BMM (T) moves individuals to the landward extreme of the domain, resulting in high entrainment losses for most source regions in the Delta, including ones that are distant from the export facilities. BMM T predicts lower entrainment for regions with terminal ends, such as Napa and Suisun Marsh. The remaining BMMs include tidal migration when triggered by a salinity cue. These conditional tidal migration BMMs result in good retention in the Delta and Suisun Bay. However, predicted fates vary among these BMMs with the largest entrainment for TpsHt. In all movement models, the majority of particles released in the South Delta (sdelta) are entrained, suggesting that none of these behaviors offers a mechanism to escape entrainment once they enter the South Delta. Note that the South Delta and many other source regions in Figure 10 are associated with low abundance, based on the FMWT survey data (Table 1). The most relevant source regions are "sac_sherm" and "sac_rio," which contain the majority of catch of Delta Smelt at the start of the simulation based on the FMWT catch data.

Although Figure 10 shows predicted fates for particles released in each source region, it does not directly provide estimates of fate or

https://doi.org/10.15447/sfews.2021v19iss1art3

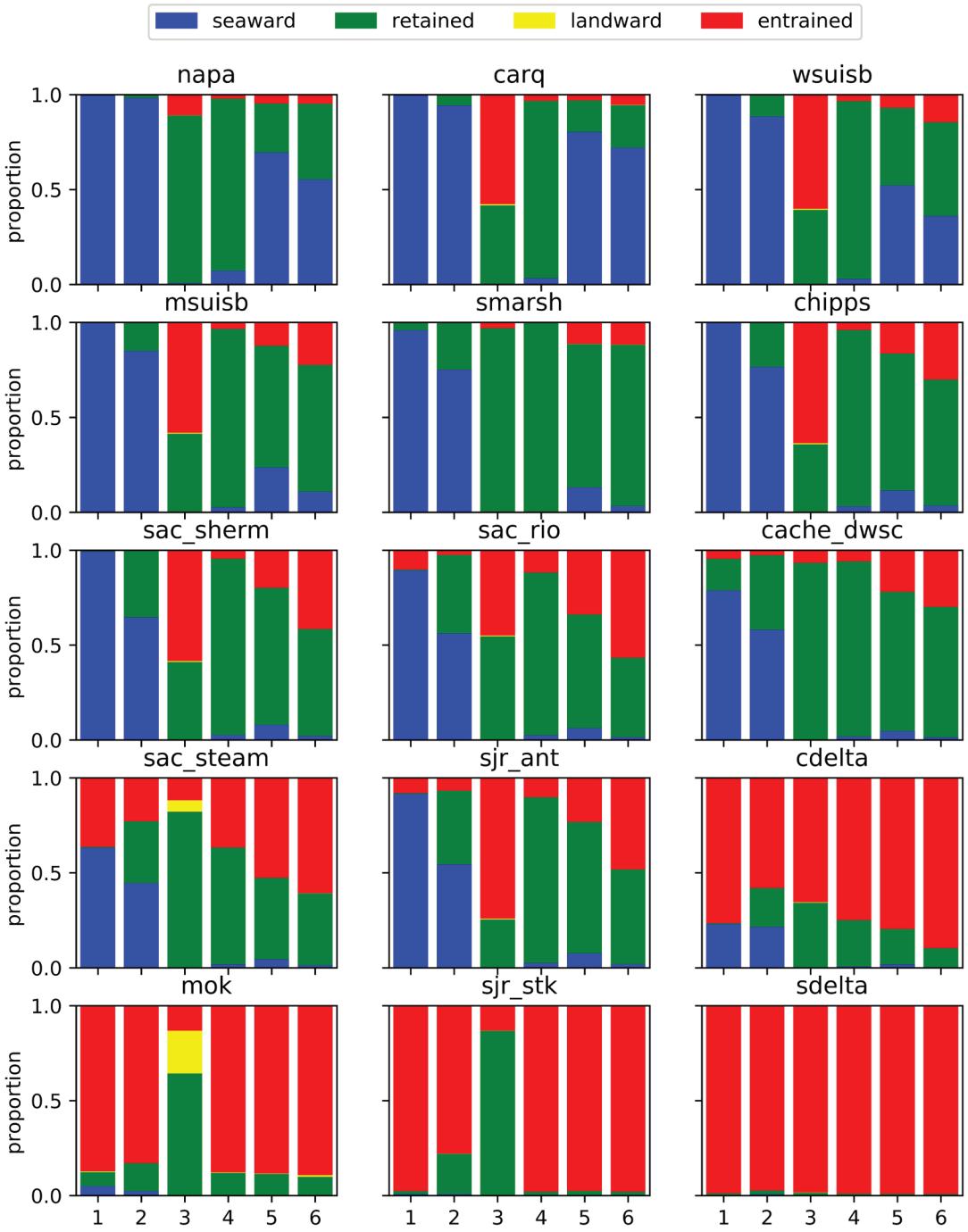

Figure 10 Fates of particles on April 17, 2002 for each release region (*panel*) and behavior (*columns in panel*) after 133 days of particle movement. The codes on the x-axes correspond to the behaviors listed in Table 2. The *colors in each bar* show the proportion of individual particles classified "seaward" if they are seaward of the defined regions in Figure 2, "retained" if located inside any of the defined regions, "landward" if located in the Delta but outside of the defined regions, and "entrained" if they entered export facilities.

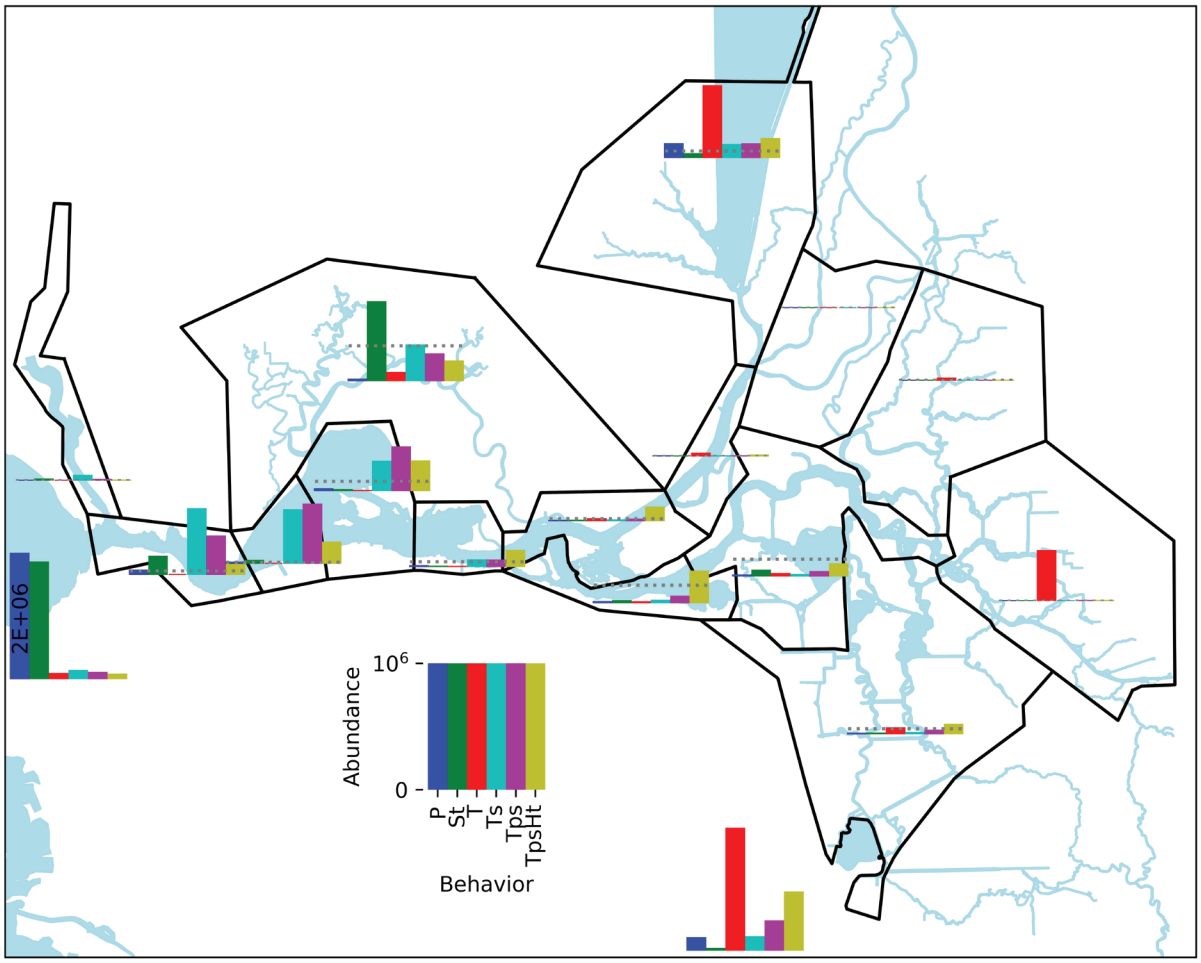

Figure 11 Predicted regional abundance for each behavior-driven movement model (BMM) (see Table 2) at the time of the first Spring Kodiak Trawl (SKT) survey from January 7 through 10, 2002. Estimated seaward losses at that time are shown at the far left, and entrainment losses at the bottom near the export facilities. The estimated regional abundances based on SKT catch observations are shown with dashed lines.

distribution of the Delta Smelt population because the population is not uniformly distributed among source regions at the start of the simulation. We predict the distribution of Delta Smelt for each BMM using Equation 5 and the FMWT data to infer an initial Delta Smelt distribution. We then compare the regional distribution for the first SKT survey, on January 7, 2002, predicted by each BMM, with regional abundances estimated from expansion of average SKT catch per unit effort over each region's habitat volume (Figure 11). The predicted regional abundances from Equation 5 vary greatly among BMMs. Passive (P) and turbidity-seeking (St) predict high domain losses and low entrainment losses. This leads to under-predictions of abundance compared with estimates from the SKT data. BMM T predicts a large landward shift in distribution and the highest entrainment losses of any BMM. The remaining BMMs—all of which include tidal migration conditional on salinity conditions—predict intermediate distributions that are more consistent with SKT-based estimates of distribution, with substantial abundance from Suisun Bay through the Central Delta and lower entrainment losses than tidal migration (T). The distribution of BMM TpsHt extended furthest into the Central and South Delta relative to the other conditional tidal migration behaviors (Ts and Tps).

https://doi.org/10.15447/sfews.2021v19iss1art3

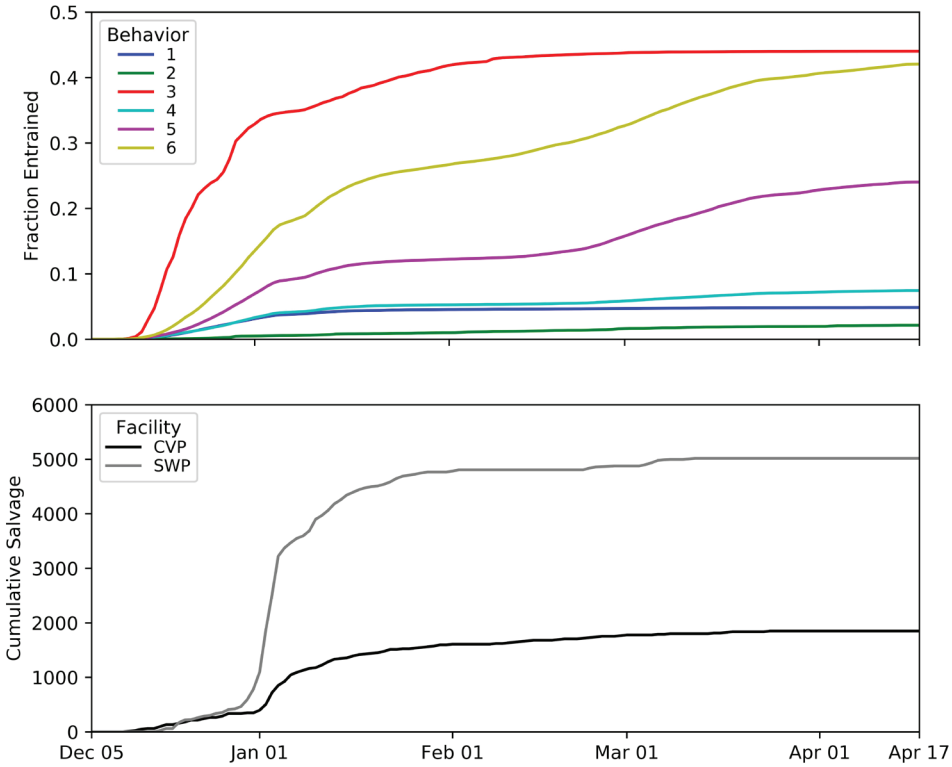

Figure 12 (**A**) Predicted fraction of Delta Smelt entrained in export facilities for each behavior-driven movement model (BMM), and (**B**) cumulative observed Delta Smelt salvage reported at each facility

The predicted timing and magnitude of entrainment varied widely among BMMs (Figure 12). The BMMs with poor retention, passive (P), and turbidity-seeking (St), predict low entrainment limited to early in the simulation period, which is not consistent with observed salvage. The largest entrainment is predicted for BMM T and occurs early in the simulation period with insignificant entrainment predicted later in the simulation period. Among the more complex behaviors (Tps and TpsHt), substantial differences in entrainment are predicted, with higher entrainment for TpsHt. Both predict entrainment in March and April when virtually no salvage was observed. Note that the fraction entrained is not equivalent to proportional entrainment losses because natural mortality is not considered in the estimate of fraction of individuals entrained shown in Figure 12. Proportional entrainment losses are estimated in Korman et al. (this volume).

A large shift in distribution is evident between the initial distribution and the first SKT survey (Figure 13). During this time, the predicted distribution for BMM TpsHt shifts from initial presence dominantly in the sac_sherm and sac_rio regions to a broader distribution, including substantial predicted abundance in the cdelta and sjr_ant regions. The abundance summed across regions decreases in time as a result of application of daily survival in the predictions, domain losses, and entrainment. The BMM TpsHt generally predicts higher abundance in regions with higher abundance calculated from SKT catch data. Regions with zero or low catch generally are also predicted to have low abundance. The regions with higher estimated abundance also show significant variability in SKT catch rates across stations. This indicates there is considerable uncertainty in catch-based abundance estimates. Given this uncertainty, predicted regional abundances are partially consistent with SKT data.

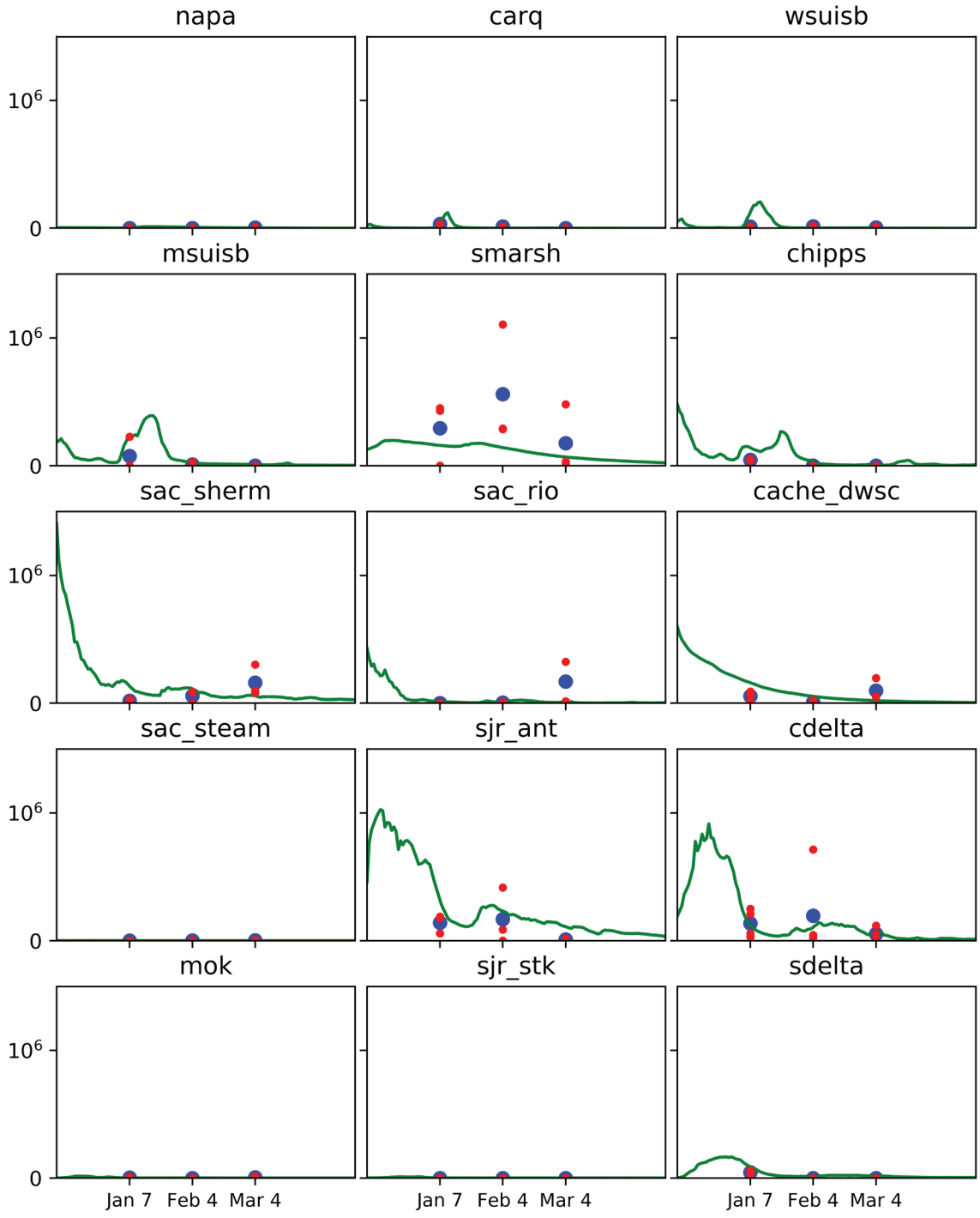

Figure 13 Estimated Delta Smelt regional abundance based on SKT surveys using all stations in each region (*blue circles*) and individual stations (*red circles*). *Green lines* show predicted daily regional abundance for behavior-driven movement model (BMM) TpsHt beginning December 5, 2001 and ending April 17, 2002.

https://doi.org/10.15447/sfews.2021v19iss1art3

DISCUSSION

Our study shows that hypothesized adult Delta Smelt swimming behaviors (e.g., Sommer et al. 2011; Bennett and Burau 2015) produce a large range of predicted distributions, and that some BMMs with increased complexity more consistently reproduced distributions evident in SKT catch data. The distribution of passive particles was not consistent with SKT survey data. The TpsHt BMM produced distributions most consistent with SKT observations qualitatively (Figure 11) and quantitatively (Korman et al. this volume). This behavior used both salinity and turbidity as environmental stimuli. Increasing perceived salinity change was the stimulus to initiate tidal migration, while turbidity resulted in a holding behavior that increased retention. This is broadly consistent with previous conclusions that observed Delta Smelt presence is related to both salinity and turbidity (Feyrer et al. 2013). However, this and other top-ranked behaviors also had some persistent biases. Notably, more Delta Smelt were predicted in the South Delta for the TpsHt BMM than indicated by catch. This may translate to an over-prediction of entrainment losses for that behavior.

All of the best-rated behaviors in the evaluation of Korman et al. (this volume) included a tidal migration behavior conditional on salinity conditions for Delta Smelt, and one included an additional turbidity response. The use of salinity to drive behavior is consistent with the approach used in Rose et al. (2013), and the salinity-based BMMs produced distributions that fit data better than passive behaviors. We did not evaluate a large range of behavior rules using turbidity cues because turbidity predictions for water year 2002 were uncertain as a result of limited calibration data. The influence of turbidity on behavior may be particularly critical in the South Delta, where predicted turbidity was low in 2002 (Figure 8). The greater success of behaviors using salinity cues alone than behaviors using turbidity cues alone to predict spatial distribution was unexpected, since Delta Smelt catch is strongly associated with higher turbidity (Moyle et al. 1992; Feyrer et al. 2007; Sommer and Mejia 2013). Decreased predation on Delta Smelt in higher-turbidity water, or reduced catchability in clear water, may be partially responsible for the observed relationship between catch and turbidity (see Korman et al., this volume). As described below, additional work is needed to examine uncertainties related to behavior and turbidity cues.

The results reported here provide inferences on entrainment losses. Estimated particle entrainment varies greatly among BMMs, suggesting that uncertainty in swimming behavior leads to uncertainty in estimated entrainment. This also implies that Delta Smelt behavioral responses to environmental cues influence entrainment losses. Retention in the estuary is a prerequisite for substantial entrainment of individuals initially near the Sacramento-San Joaquin confluence region. BMMs with tidal migration in high or increasing salinity generally had good retention, allowing the possibility of substantial entrainment. Predicted particle entrainment varies greatly among particle-release locations, with higher entrainment for particles released closer to exports. The magnitude of flow through OMR toward export facilities also influences entrainment. Gross et al. (2018) predicted greatly reduced entrainment for water year 2002 using RPA flow restrictions instead of historical flows.

Because salinity is a conservative water-quality constituent that varies smoothly in the estuary, it can be expected that tidal migration driven by a salinity threshold will lead to substantial retention landward of that salinity threshold. In contrast, turbidity is more heterogeneous and unsteady as a result of local settling and re-suspension, local turbidity maxima, and junction dynamics in the Delta, and is, thus, more challenging to predict accurately. Therefore, inconsistencies in predicted and observed spatial distributions of Delta Smelt for turbidity-based BMMs could be caused by error in turbidity predictions that drive the predictive behavior, in addition to uncertainty in the prescribed behavior.

Several simplifications of the behavior-driven approach taken in this study may be biologically unrealistic. Specifying and testing biologically realistic rules may require additional knowledge of the sensory abilities of Delta Smelt. For example, the actual perceived intensity of an environmental stimulus, such as velocity shear or salinity, may have a logarithmic or other non-linear relationship to stimulus (Goodwin et al. 2014). Furthermore, in the current formulation, the perceived change in intensity of a stimulus (Equation 4) may cause a behavior response for a small relative change in an environmental stimulus. For example, BMM Tps may result in tidal migration in low-salinity conditions from a relative change in salinity, such as a change from 0.1 psu to 0.2 psu. The larger entrainment predicted for Tps relative to Ts results from tidal migration at lower salinity values for Tps than the 1 psu threshold for tidal migration in Ts. We do not know if Delta Smelt can perceive and respond to these small changes in salinity.

The larger set of BMMs explored in Gross et al. (2018) yielded either poorer results or no improvement with increased complexity relative to TpsHt. However, it is likely that all representations of behavior included were, at best, crude representations of actual behavior. For example, none of the behaviors included stochastic components, and the only environmental stimuli considered were those predicted by the hydrodynamic and sediment-transport models. Improvements could include modified swimming parameters, a conceptually different swimming behavior, or a framework that incorporated stochasticity. Additional behaviors could include environmental stimuli that would result in homing to natal habitat. However, given the limitations of SKT and salvage observations discussed in Korman et al. (this volume), additional effort in refining BMMs may not lead to improvements in confidence. Further evaluation should involve multiple years of comparisons to SKT and salvage data to establish whether the relative performance of BMMs is consistent year to year.

The Delta Smelt distribution and entrainment results here are conditional on the hydrodynamic and sediment-transport results. These were produced by a well-documented and published 3-D model (e.g., MacWilliams et al. 2015; Bever et al. 2018). However, it is possible the results have some sensitivity to model resolution. In particular, the efficacy of tidal migration depends on lateral differences in velocity between the channel and shoreline. Increased model resolution would allow particles to find more quiescent near-shore regions, increasing the effectiveness of tidal migration behaviors. To improve the predicted turbidity throughout the Delta, additional work should use spatially-varying suspended-sediment concentration-to-turbidity curves in sediment-transport modeling.

If, upon further refinement of the turbidity and Delta Smelt behavior-driven modeling approach, one or more behavior fits the data for multiple water years, the modeling and statistical approach developed for this project could be used to anticipate conditions of entrainment risk, possibly in real time. The modeling and statistical approach developed for this project can also readily be applied to evaluate hypothesized behavior of other species in the estuary, to the extent that the distribution of those species is well represented by survey data. To avoid uncertainties introduced by low catch, this effort is best performed using data from when the species studied were abundant. Once confidence is established in representation of behavior by comparing predicted distribution to catch from a high-abundance year, the BMM could then be applied in lower-abundance conditions.

ACKNOWLEDGEMENTS

Funding for this study was provided by the United States Bureau of Reclamation, State and Federal Contractors Water Agency, and the California Department of Water Resources through the Collaborative Science Adaptive Management Program (CSAMP). Additional funding was provided by the US Fish and Wildlife Service. This study was done under the direction of CSAMP's Collaborative Adaptive Management

Team (CAMT) and the Delta Smelt Scoping Team (DSST). Our analysis relied heavily on long-term trawl and salvage data sets. We thank Ben Saenz, Richard Rachiele and Stacie Grinbergs for contributions to modeling work. We thank Rusty Holleman for Python utilities for analysis of unstructured grid model results. We thank Scott Burdick for contributing to figure preparation. We thank the many biologists and technicians working for California Department of Fish and Wildlife, the US Fish and Wildlife Service, and the Bureau of Reclamation for the collection and maintenance of these data. We thank the DSST for providing valuable comments and discussion over the course of this project and on earlier drafts of this manuscript. The UnTRIM code was developed and provided by Professor Vincenzo Casulli (University of Trento, Italy). We would like to thank the Bundesanstalt für Wasserbau (BAW), Holger Weilbeer (BAW), and the University of the German Federal Armed Forces for their collaboration on the use of the SediMorph model. Viewpoints expressed in this manuscript are those of the authors and do not reflect the opinions of the California Department of Water Resources.

REFERENCES

Baxter R, Breuer R, Brown L, Conrad L, Feyrer F, Fong S, Gehrts K, Grimaldo L, Herbold B, Hrodey P, et al. 2010. Interagency Ecological Program 2010 Pelagic Organism Decline work plan and synthesis of results. Sacramento (CA): Interagency Ecological Program for the San Francisco Estuary. 259 p. [accessed 2021 Jan 07]. Available from: *https://www.waterboards.ca.gov/waterrights/water_issues/programs/bay_delta/docs/cmnt091412/sldmwa/baxter_etal_iep_2010.pdf*

Bennett WA, Burau JR. 2015. Riders on the storm: selective tidal movements facilitate the spawning migration of threatened Delta Smelt in the San Francisco Estuary. Estuaries Coasts [accessed 2021 Jan 07];38:826–835. *https://doi.org/10.1007/s12237-014-9877-3*

Bever AJ, MacWilliams ML. 2013. Simulating sediment transport processes in San Pablo Bay using coupled hydrodynamic, wave, and sediment transport models. Mar Geol. [accessed 2021 Jan 07];345:235-253. *https://doi.org/10.1016/j.margeo.2013.06.012*

Bever AJ, MacWilliams ML, Fullerton DK. 2018. Influence of an observed decadal decline in wind speed on turbidity in the San Francisco Estuary. Estuaries Coasts. [accessed 2021 Jan 07];41:1943-1967. *https://doi.org/10.1007/s12237-018-0403-x*

Binder TR, Cooke SJ, Hinch SG. 2011. Fish migrations | the biology of fish migration. In: Farell AP, editor. Encyclopedia of fish physiology: from genome to environment. San Diego (CA): Academic Press. p. 1921-1927. [accessed 2021 Jan 07]. Available from: *https://www.sciencedirect.com/referencework/9780080923239/encyclopedia-of-fish-physiology*

[BAW] Bundesanstalt für Wasserbau (German Federal Waterways Engineering and Research Institute), 2005. Mathematical Module SediMorph, Validation Document – Version 1.1. Karlsruhe (Germany): BAW. 77 p. [accessed 2021 Jan 07]. Available from: *https://wiki.baw.de/downloads/wasserbau/mathematische_verfahren/pdf/vd-sedimorph.pdf*

[CDWR] California Department of Water Resources. 2016. Chronological reconstructed Sacramento and San Joaquin Valley water year hydrological classification indices. [accessed 2021 Jan 07]. Available from: *http://cdec.water.ca.gov/cgi-progs/iodir/wsihist*

Cheng RT, Casulli V, Gartner JW. 1993. Tidal, residual, intertidal mudflat (TRIM) model and its application to San Francisco Bay, California. Estuar Coast Shelf Sci. [accessed 2021 Jan 07];36:235–280. *https://doi.org/10.1006/ecss.1993.1016*

Feyrer F, Nobriga M, Sommer T. 2007. Multi-decadal trends for three declining fish species: habitat patterns and mechanisms in the San Francisco Estuary, California, U.S.A. Can J Fish Aquat Sci. [accessed 2021 Jan 07];136:1393–1405. *https://doi.org/10.1139/F07-048*

Feyrer F, Portz D, Odum D, Newman KB, Sommer T, Contreras D, Baxter R, Slater SB, Sereno, D, Van Nieuwenhuyse. 2013. SmeltCam: underwater video codend for trawled nets with an application to the distribution of the imperiled Delta Smelt. PLoS ONE. [accessed 2021 Jan 07];8(7):e67829. *https://doi:10.1371/journal.pone.0067829*

Ganju NK, Schoellhamer DH. 2009. Calibration of an estuarine sediment transport model to sediment fluxes as an intermediate step for simulation of geomorphic evolution. Cont Shelf Res. [accessed 2021 Jan 07];29(1):148–158. *https://doi.org/10.1016/j.csr.2007.09.005*

Goodwin RA, Politano M, Garvin JW, Nestler JM, Hay D, Anderson JJ, Weber LJ, Dimperio E, Smith DL, Timko MA. 2014. Fish navigation of large dams emerges from their modulation of flow field experience. Proc Natl Acad Sci. [accessed 2021 Jan 07];111:5277-5282. *https://doi.org/10.1073/pnas.1311874111*

Gräwe U, Deleersnijder E, Shah SHAM, Heemink AW. 2012. Why the Euler scheme in particle-tracking is not enough: the shallow sea test case. Ocean Dyn. [accessed 2021 Jan 07];62:501–514. *https://doi.org/10.1007/s10236-012-0523-y*

Grimaldo L, Sommer T, Van Ark N, Jones G, Holland E, Moyle P, Smith P, Herbold, B. 2009. Factors affecting fish entrainment into massive water diversions in a freshwater tidal estuary: can fish losses be managed? N Am J Fish Manag. [accessed 2021 Jan 07];29:1253-1270. *https://doi.org/10.1577/M08-062.1*

Gross, ES, Saenz, B, Rachiele, R, Grinbergs, S, Grimaldo, LF, Korman, J, Smith, PE, MacWilliams M, Bever A. 2018. Estimation of adult Delta Smelt distribution for hypothesized swimming behaviors using hydrodynamic, suspended sediment and particle-tracking models. Walnut Creek (CA): Resource Management Associates. Technical Report DWR-1249. 58 p. [accessed 2021 Jan 07]. Available from: *https://www.waterboards.ca.gov/waterrights/water_issues/programs/bay_delta/california_waterfix/exhibits/docs/petitioners_exhibit/dwr/part2_rebuttal/dwr_1249.pdf*

Hobbs JA, Lewis LS, Willmes M, Denney C, Bush E. 2019. Complex life histories discovered in a critically endangered fish. Sci Rep. [accessed 2021 Jan 07];9:16772. *https://doi.org/10.1038/s41598-019-52273-8*

Honey K, Baxter R, Hymanson Z, Sommer T, Gingras M, Cadrett P. 2004. IEP long-term fish monitoring program element review. Sacramento (CA): Interagency Ecological Program of the Sacramento-San Joaquin Estuary. Technical Report 78. [accessed 2021 Jan 07]. 220 p. Available from: *https://www.academia.edu/507408/IEP_long_term_fish_monitoring_program_element_review*

Ketefian GS, Gross ES, Stelling GS. 2016. Accurate and consistent particle tracking on unstructured grids. Int J Num Meth Fluids. [accessed 2021 Jan 07];80:648-665. *https://doi.org/10.1002/fld.4168*

Kimmerer WJ. 2008. Losses of Sacramento River Chinook Salmon and Delta Smelt to entrainment in water diversions in the Sacramento-San Joaquin Delta. San Franc Estuary Watershed Sci. [accessed 2021 Jan 07];6(2). *https://doi.org/10.15447/sfews.2008v6iss2art2*

Kimmerer WJ. 2011. Modeling Delta Smelt losses at the South Delta export facilities. San Franc Estuary Watershed Sci. [accessed 2021 Jan 07];9(1). *https://doi.org/10.15447/sfews.2011v9iss1art3*

Korman J, Gross ES, Grimaldo LF. 2021. Statistical evaluation of behavior and population-dynamic models that predict movement and proportional entrainment loss of adult Delta Smelt in the Sacramento-San Joaquin River Delta. San Franc Estuary Watershed Sci. [DOI]

Leggett WC. 1977. The ecology of fish migrations. Ann Rev Ecol Syst. [accessed 2021 Jan 07];8:285-308. *https://doi.org/10.1146/annurev.es.08.110177.001441*

MacWilliams M, Bever A, Gross E, Ketefian G, Kimmerer W. 2015. Three-dimensional modeling of hydrodynamics and salinity in the San Francisco Estuary: an evaluation of model accuracy, X2, and the Low-Salinity Zone. San Franc Estuary Watershed Sci. [accessed 2021 Jan 07];13(1). *https://doi.org/10.15447/sfews.2015v13iss1art2*

Malcherek A. 2001. Hydromechanik der Fließgewässer (Hydromechanics of Rivers). Hanover (FRG): Institut für Strömungsmechanik and Elektronisches Rechen im Bauwesen der Universität. (University of Hanover Institute of Fluid Mechanics and Electronic Computing in Building). Bericht Nr. 61 (Report No. 61). [accessed 2021 Jan 07]. 382 p. Available from: *https://books.google.com/books/about/Hydromechanik_der_Flie%C3%9Fgew%C3%A4sser.html?id=7SwNuAAACAAJ*

Malcherek, A, Knock D. 2006. The influence of waves on the sediment composition in a tidal bay. In: Spaulding ML, editor. Proceedings of the Ninth International Conference on Estuarine and Coastal Modeling; 2005 October 31–September 2; Charleston. Reston (VA): ASCE. [accessed 2021 Jan 07]. p. 842–859. Available from: *https://doi.org/10.1061/40876(209)48*

Miller WJ. 2011. Revisiting assumptions that underlie estimates of proportional entrainment of Delta Smelt by state and federal water diversions from the Sacramento-San Joaquin Delta. San Franc Estuary Watershed Sci. [accessed 2021 Jan 07];9(1). *https://doi.org/10.15447/sfews.2011v9iss1art2*

Mil'shtejn GN. 1974. Approximate integration of stochastic differential equations. Theory Probab Appl. [accessed 2021 Jan 07];19:557–562. *https://doi.org/10.1137/1119062*

Moyle PB, Herbold B, Stevens DE, Miller LW. 1992. Life history and status of Delta Smelt in the Sacramento–San Joaquin Estuary, California. Trans Am Fish Soc. [accessed 2021 Jan 07];121:67–77. *https://doi.org/10.1577/1548-8659(1992)121<0067:LHASOD>2.3.CO;2*

Murphy DD, Hamilton, SA. 2013. Eastward migration or marshward dispersal: exercising survey data to elicit an understanding of seasonal movement of Delta Smelt. San Franc Estuary Watershed Sci. [accessed 2021 Jan 07];6(1). *https://doi.org/10.15447/sfews.2013v11iss3art12*

Nobriga ML, Sommer TR, Feyrer F, Fleming K. 2008. Long-term trends in summertime habitat suitability for Delta Smelt, *Hypomesus transpacificus*. San Franc Estuary Watershed Sci. [accessed 2021 Jan 07];11(3). *https://doi.org/10.15447/sfews.2008v6iss1art1*

Paris C, Chérubin L, Cowen R. 2007. Surfing, spinning, or diving from reef to reef: effects on population connectivity. Mar Ecol Prog Ser. [accessed 2021 Jan 07];347:285–300. *https://doi.org/10.3354/meps06985*

Polansky L, Newman KB, Nobriga ML, Mitchell L. 2017. Spatiotemporal models of an estuarine fish species to identify patterns and factors impacting their distribution and abundance. Estuaries Coasts. [accessed 2021 Jan 07];41:572–581. *https://doi.org/10.1007/s12237-017-0277-3*

Rose KA, Kimmerer WJ, Edwards KP, Bennett WA. 2013. Individual-based modeling of Delta Smelt population dynamics in the upper San Francisco Estuary: I. Model description and baseline results. Trans Am Fish Soc. [accessed 2021 Jan 07];142:1238–1259. *https://doi.org/10.1080/00028487.2013.799518*

Secor HD, Rooker JR. 2000. Is otolith strontium a useful scalar of life cycles in estuarine fishes? Fisheries Research. [accessed 2021 Jan 07];46:359-371. *https://doi.org/10.1016/S0165-7836(00)00159-4*

Shah SHAM, Heemink AW, Gräwe U, Deleersnijder E. 2013. Adaptive time stepping algorithm for Lagrangian transport models: theory and idealized test cases. Ocean Model. [accessed 2021 Jan 07];68:9-21. *https://doi.org/10.1016/j.ocemod.2013.04.001*

Sommer T, Armor C, Baxter R, Breuer R, Brown L, Chotkowski M, Culberson S, Feyrer F, Gingras M, Herbold B, et al. 2007. The collapse of pelagic fishes in the upper San Francisco Estuary. Fisheries. [accessed 2021 Jan 07];32(6):270–277. *https://doi.org/10.1577/1548-8446(2007)32[270:TCOPFI]2.0.CO;2*

Sommer T, Mejia F, Nobriga M, Feyrer F, Grimaldo L. 2011. The spawning migration of Delta Smelt in the upper San Francisco Estuary. San Franc Estuary Watershed Sci. [accessed 2021 Jan 07];9(2). *https://doi.org/10.15447/sfews.2014v9iss2art2*

Sommer T, Mejia F. 2013. A place to call home: a synthesis of Delta Smelt habitat in the upper San Francisco Estuary. San Franc Estuary Watershed Sci. [accessed 2021 Jan 07];11(2). *https://doi.org/10.15447/sfews.2013v11iss2art4*

SWAN Team. 2009. SWAN user manual version 40.72. Delft (Netherlands): Delft University of Technology. [accessed 2021 Jan 07]. Available from: *https://manualzilla.com/doc/5813978/user-manual-swan-cycle-iii-version-40.72a*

Swanson C, Young PS, Cech JJ Jr. 1998. Swimming performance of Delta Smelt: maximum performance, and behavioral and kinematic limitations on swimming at submaximal velocities. J Exp Biol. [accessed 2021 Jan 07];201:333–345. Available from: *https://jeb.biologists.org/content/201/3/333*

Tsukamoto K, Miller MJ, Kotake A, Aoyama J, Uchida K. 2009. The origin of fish migration: the random escapement hypothesis. Am Fish Soc Symp. [accessed 2021 Jan 07];69:45-61. Available from: *https://www.researchgate.net/publication/313511464_The_origin_of_fish_migration_the_random_escapement_hypothesis*

[USGS] US Geological Survey. 2015. National Water Information System. [accessed 2015 Jul 1]. Available from: *http://waterdata.usgs.gov/ca/nwis*

[USFWS] US Fish and Wildlife Service. 2008. 2008 Biological Opinion for Delta Smelt. [accessed 2015 Jul 1]. Sacramento (CA): USFWS, California and Nevada Region. Available from: *https://www.fws.gov/sfbaydelta/documents/SWP-CVP_OPs_BO_12-15_final_OCR.pdf*

van der Wegen M, Jaffe BE, Roelvink JA. 2011. Process-based, morphodynamic hindcast of decadal deposition patterns in San Pablo Bay, California, 1856-1887. J Geophy Res. [accessed 2021 Jan 07];116:F2. *https://doi.org/10.1029/2009JF001614*

Walsh CT, Reinfilds IV, Ives MC, Gray CA, West RJ, van der Meulen DE. 2013. Environmental influences on the spatial ecology and spawning behavior of an estuarine-resident fish, Macquaria colonorum. Estuar Coast Shelf Sci. [accessed 2021 Jan 07];118:60-71. *https://doi.org/10.1016/j.ecss.2012.12.009*

Wright SA, Schoellhamer DH. 2005. Estimating sediment budgets at the interface between rivers and estuaries with application to the Sacramento-San Joaquin River Delta. Water Resour Res. [accessed 2021 Jan 07];4:W09428. *https://doi.org/10.1029/2004WR003753*